

Video Article

A *Drosophila* Model to Study Wound-induced Polyploidization

Erin C. Bailey^{*1}, Ari S. Dehn^{*1}, Kayla J. Gjelsvik², Rose Besen-McNally¹, Vicki P. Losick¹

¹Biology Department, Boston College

²Graduate School of Biomedical Sciences and Engineering and Kathryn W. Davis Center for Regenerative Biology and Medicine, MDI Biological Laboratory, University of Maine

*These authors contributed equally

Correspondence to: Vicki P. Losick at vicki.losick@bc.edu

URL: <https://www.jove.com/video/61252>

DOI: [doi:10.3791/61252](https://doi.org/10.3791/61252)

Keywords: Developmental Biology, Issue 160, wound healing, tissue repair, endoreplication, polyploidy, Myc, *Drosophila*

Date Published: 6/9/2020

Citation: Bailey, E.C., Dehn, A.S., Gjelsvik, K.J., Besen-McNally, R., Losick, V.P. A *Drosophila* Model to Study Wound-induced Polyploidization. *J. Vis. Exp.* (160), e61252, doi:10.3791/61252 (2020).

Abstract

Polyploidy is a frequent phenomenon whose impact on organismal health and disease is still poorly understood. A cell is defined as polyploid if it contains more than the diploid copy of its chromosomes, which is a result of endoreplication or cell fusion. In tissue repair, wound-induced polyploidization (WIP) has been found to be a conserved healing strategy from fruit flies to vertebrates. WIP has several advantages over cell proliferation, including resistance to oncogenic growth and genotoxic stress. The challenge has been to identify why polyploid cells arise and how these unique cells function. Provided is a detailed protocol to study WIP in the adult fruit fly epithelium where polyploid cells are generated within 2 days after a puncture wound. Taking advantage of *D. melanogaster's* extensive genetic tool kit, the genes required to initiate and regulate WIP, including Myc, have begun to be identified. Continued studies using this method can reveal how other genetic and physiological variables including sex, diet, and age regulate and influence WIP's function.

Introduction

Drosophila melanogaster is an attractive model system to study the cellular and molecular mechanisms of epithelial wound repair. As in mammals, the tissue repair mechanisms used depend on both the tissue and its developmental stage. Scarless wound healing occurs in the fruit fly embryo where an actomyosin "purse string" forms at the epithelial leading edge enabling the wound to seamlessly close^{1,2}. Post-embryonic wound healing in larvae, pupae, and adult fruit flies results in extracellular matrix remodeling, melanin scar formation, and epithelial cell growth^{3,4,5,6}. The epithelial cells increase in size by cell fusion and the endocycle, an incomplete cell cycle that bypasses mitosis^{3,4,7,8}. As a result, cell loss is compensated by polyploid cell growth instead of cell division. The adult fly hindgut, midgut, and follicular epithelium also rely on polyploid cell growth to compensate for cell loss after tissue damage^{9,10,11}.

Polyploidy is a well-known aspect of organismal development in plants and insects, but in the last few years it has become more apparent that polyploidy is a conserved tissue repair strategy in vertebrates¹². The zebrafish, which has the capacity to regenerate its heart, relies on polyploid cell growth to heal damaged epicardium¹³. Polyploidy also contributes to mammalian liver regeneration and kidney tubule epithelium repair after acute injury^{14,15}. In these examples, polyploid cells are generated by endoreplication via either endocycle or endomitosis, which results in a binucleated cell due to a block in cytokinesis¹². The enigma is why polyploid cells arise during wound repair and how polyploidy affects tissue function. Recent studies have provided new insight into the question of whether polyploidy offers a healing advantage or disadvantage. In zebrafish epicardium, polyploidy enhanced the speed of wound healing¹³. In *D. melanogaster* hindgut and mammalian liver, polyploidy was found to be protective against oncogenic growth^{11,14}. In adult fly epithelium, it was recently found that polyploidy enables wound repair in the presence of genotoxic stress¹⁶. Endoreplication is resistant to DNA damage, allowing wound healing when cell proliferation would otherwise be compromised¹⁷. For cardiomyocytes in mouse and zebrafish hearts, however, polyploidy slows healing, resulting in enhanced scar formation^{18,19}. Therefore, depending on the organ and/or cell type, polyploidy can be a beneficial or detrimental tissue repair strategy. The accessibility of *D. melanogaster* genetics coupled with analysis of the wound-induced polyploidization (WIP) response make it an ideal model system for elucidating the molecular and cellular mechanisms that guide this wound healing strategy.

Here, we present a protocol for analyzing WIP in the adult *D. melanogaster* epithelium. Included are instructions for fruit fly injury, dissection, immunostaining, mounting, imaging, and analysis of re-epithelialization, cell fusion, and endoreplication (ploidy). The imaging and ploidy analysis can also be adapted to other models to test whether WIP occurs. It should be noted that with an increase in nuclear DNA content there is often a corresponding increase in nuclear size. However, there are many examples in biology where nuclear size does not reflect a corresponding change in ploidy²⁰. Even more caution should be taken when interpreting nuclear size in the context of a wound environment where cells will often spread or stretch to cover the wound site. Therefore, the only definitive proof of change in ploidy is to measure DNA content by this method (or others, such as whole genome sequencing)²¹. This method increases the suitability of the adult *D. melanogaster* abdominal epithelium as a model to study the role and regulation of polyploidy in wound repair.

Protocol

1. Staging and wounding of adult fruit flies

1. Select *D. melanogaster* strain of choice (i.e., epi-Gal4/ UAS strain, see **Table of Materials**).
NOTE: Here, the Gal4/UAS system is used to enable epithelial specific gene expression (epi-Gal4) of a gene or RNAi encoded downstream of UAS. This study uses fluorescent membrane protein (UAS-Cd8.mRFP), mitotic inducer (UAS-fzr^{RNAi}, UAS-stg), and WIP inhibitor (UAS-E2F1^{RNAi}, UAS-Rac^{DN}).
2. Collect two vials of 10-15 newly enclosed female fruit flies each and age on fresh food vials at 25 °C until 3-5 days old. One vial will serve as the uninjured control and the other vial will be wounded as described below. The female flies should be maintained with males (~5/vial).
3. To wound the flies, assemble several pin holders each with a single 0.10 mm stainless steel pin. Ensure the sharp end of the pin is facing out. Pins can easily bend or chip after puncturing the fly and hooked or damaged pins should be discarded.
4. Anesthetize aged female fruit flies on a CO₂-fly pad under a stereomicroscope and align them into a row using a paint brush. Wearing safety glasses, holding the pin holder in one hand and forceps in the other, use forceps to position a fly with its ventral abdomen facing up.
5. Puncture the adult female flies within the epithelial pleurite region of tergite A4 on either side of the ventral midline sternites (**Figure 1A**). Puncturing this ventral region provides optimal space away from the dissection sites where tissue edges will be torn by mechanical processing.
6. Return wounded flies to the food vial and age to desired day post injury (dpi). Epithelial wound healing starts at 1 dpi and ends by 3 dpi. Endoreplication peaks at 2 dpi, which is ideal for the EdU assay (section 4, **Figure 2**).

2. Fly abdominal dissection

NOTE: During this step, it is important to avoid touching the ventral abdominal tissue with the dissection tools because it will compromise the integrity of the epithelium.

1. Obtain all required materials for dissection: Grace's solution, forceps, Vanna's Spring Scissors, 0.10 mm pins, dissecting plates, 9 well glass dissection dish, fixative solution (4% paraformaldehyde in 1x PBS), 1x PBS, wipes, pipettes and tips for 30 µm, and gloves (see **Table of Materials**).
2. Confirm that flies were successfully injured by anesthetizing wounded flies on a CO₂-fly pad under a stereomicroscope and checking for the presence of the wound scar (i.e., a melanin spot on abdomen, see **Figure 1B**). Discard any flies from the experimental group that were not successfully wounded.
3. To start dissection, fill one well of a 9 well glass dissection dish with Grace's solution. Use a pair of forceps to grasp a wounded female fly by the dorsal side of the thorax and submerge the fly in the well containing Grace's solution.
4. Using forceps in the opposite hand without releasing the thorax, puncture the dorsal cuticle below tergite A6 and pull the cuticle off the rear end of the fruit fly. The internal organs (ovary and intestine) will usually come out at this step. If not, gently push on the dorsal side of the abdomen with the forceps to squeeze out the remaining organs and discard into an empty well.
5. Snap off the full abdomen at the thorax junction above tergite A2 using the forceps and transfer the abdomen to an empty well containing ~100 µL of Grace's solution.
6. Repeat steps 2.3-2.5 until all fly abdomens are dissected.
7. Reduce the volume of Grace's solution to 30 µL in the well containing pooled, dissected abdomens.
8. Fillet the abdomens open by positioning the abdomen on the dorsal side with the forceps in one hand and then inserting the bottom blade of Vanna's spring scissors into the abdominal cavity with the other hand. Cut along the dorsal midline until the abdomen is fully opened, which can require up to three cuts (**Figure 1C, 1D**).
9. Set up a dry dissecting plate with four 0.10 mm pins per abdominal mounting area. Each 35 mm dissecting plate can fit up to seven mounting areas. Pipette 30 µL of Grace's solution on each mounting area and transfer one filleted abdomen to each droplet.
10. Pin the filleted abdomens to the dish on the four dorsal corners (**Figure 1E**). Ensure that the tissue lies flat without tearing or overstretching the abdominal tissue.
11. To fix the tissue, pipette off the Grace's solution and add 30 µL of the fix solution to the pinned abdomen.
CAUTION: Wear gloves while handling the fix solution, as paraformaldehyde is toxic.
12. Repeat steps 2.10-2.11 until all filleted abdomens are pinned onto the dissecting plate.
13. Place a tape label on the bottom of each dish to mark each control and experimental group. Fix samples for 30-60 min at room temperature (RT).
14. Wash off fix solution by pipetting on 1.5 mL of 1x PBS to each plate. Dispose of fix solution and plastics in appropriate liquid or dry chemical waste containers according to institutional guidelines.
15. Wash plates 2x with 1.5 mL of 1x PBS and store fixed tissue covered in 1.5 mL of 1x PBS in a plastic container with a lid. Add a layer of damp paper towel to the bottom of the container and store samples at 4 °C until ready to immunostain within 1 week of dissection.

3. Immunofluorescence

1. Freshly prepare reagents (see **Table of Materials**): wash buffer solution (0.3% Triton X 100, 0.3% BSA in 1x PBS). Leftover wash buffer can be saved at 4 °C and used for the duration of the 2 day staining protocol. Prepare enough primary antibody solution per assay (**Figure 2**) using Anti-FasIII (1:50 mouse anti-Fasciilin-III) in wash buffer with either anti-Grh (1:300 affinity purified rabbit anti-Grainyhead³) or anti-RFP (1:1,000 rabbit anti-RFP). Primary antibody solutions can be saved at 4 °C and reused multiple times until signal is significantly reduced.
2. Permeabilize tissue by pipetting off 1x PBS, adding 1.5 mL of wash buffer, and incubating for at least 30 min on an orbital shaker (80 rpm) at RT.

- Remove wash buffer and stain tissue overnight with 1.5 mL of primary antibody solution, incubating on an orbital shaker (80 rpm) at 4 °C. Collect the primary antibody solution and save in a tube at 4 °C for future experiments.
- First rinse the sample quickly with 1x PBS and then wash 3x with 1.5 mL of wash buffer. For each wash, incubate samples at RT on an orbital shaker for at least 30 min.
- During the final wash, prepare the secondary antibody solution: 1:1,000 donkey anti-rabbit Alexa 488 or 568 and 1:1,000 goat anti-mouse Alexa 488 or 568 (or fluorophores of choice) in wash buffer.
- Remove wash buffer and stain tissues with 1.5 mL of secondary antibody solution. Cover samples with aluminum foil and incubate on an orbital shaker at RT for 3 h. Alternatively, samples can be incubated overnight at 4 °C on an orbital shaker.
- Wash samples by first discarding secondary antibody solution and then rinse sample quickly with 1x PBS followed by three washes with 1.5 mL of wash buffer. For each wash, incubate samples at RT on an orbital shaker for at least 30 min.
- Prepare DAPI solution by diluting DAPI to 10 µg/mL in wash buffer. After the final wash, stain samples with 1.5 mL DAPI solution incubating at RT for 30 min.
- Discard DAPI solution and rinse samples 2x in 1.5 mL of 1x PBS. Store stained tissue in 1.5 mL of 1x PBS in the dark, covered with aluminum foil, at 4 °C until ready to mount on a glass slide with coverslip. The mounting step should be performed within 1 week.

4. Cell cycle activity (EdU Assay)

- Make up a 10 mM EdU stock solution from Click-iT kit (see **Table of Materials**) by dissolving EdU powder in dH₂O and mixing for ~15 min until completely dissolved. The stock solution can be aliquoted (250 µL per tube) and stored at -80 °C.
- Feed flies EdU by first diluting EdU stock to 5 mM in dH₂O. Add dry yeast until the solution is cloudy and briefly vortex to mix. Cut off a 0.5 mL tube cap and place it at the bottom of the fly food vial. Push the cap into the food, so it is stable.
- Anesthetize the flies and transfer 3-5 day old flies into the vial. Tap the flies to one edge so none are stuck in the cap.
- Pipette 75 µL of yeast-EdU solution into the cap. Flies should be fed fresh yeast-EdU solution every day and transferred to a fresh food vial with a cap every other day to ensure that the flies do not get stuck in the bottom of the vial.
- To transfer flies, flip to a new vial with a cap, put flies to sleep, tap flies to one side, and add fresh yeast-EdU solution.
- On the third day, injure the flies and continue to feed yeast-EdU until dissection at 2 dpi (**Figure 4A**). See protocol section 2 for dissection and fixation methods.
- Prepare EdU staining reagents: wash buffer (0.3% Triton X 100, 0.3% BSA in 1x PBS), permeabilization buffer (0.5% Triton X 100 in 1x PBS), blocking buffer (3% BSA in 1x PBS), and prepare reagents from the EdU assay kit (see **Table of Materials**), including 1x reaction buffer and 1x reaction buffer additive as directed by the manufacturer.
- Wash samples for 1 h, mixing at RT in 1.5 mL of wash buffer.
- Add 1.5 mL of permeabilization buffer and incubate samples for 20 min.
NOTE: Thaw and prepare reaction cocktail solution using a volume of 500 µL/plate.
- Wash samples 1x quickly with 1x PBS and then 3x quickly with 1 mL of blocking buffer.
- Pipette off all remaining blocking buffer and add 500 µL of reaction cocktail solution per plate. Swirl plates to ensure tissues are completely covered. Incubate in a drawer in the dark for 1 h at RT.
- Wash samples 1x quickly with 1.5 mL of blocking buffer.
- Stain with 1.5 mL of DAPI solution at 1:5,000 in wash buffer for 30 min.
- Wash 2x with 1x PBS quickly, wrap in foil, and store in the dark at 4 °C until ready to mount samples within 3 days.

5. Mount stained tissue

- Obtain all required materials for mounting: glass slides, glass coverslips, clear nail polish, mounting media, a pair of forceps, and wipes.
- To mount stained fly tissue, unpin abdomens from the dissecting plate using forceps under the stereomicroscope. Transfer tissue to ~30 µL of mounting media on a glass coverslip by gently grabbing the tissue with forceps by its dorsal flanks, taking care to avoid touching the ventral area with forceps.
- Under the stereomicroscope orient the abdominal tissue so that the inside is facing down toward the coverslip (i.e., the external cuticle/bristles are facing up). Pull the oriented abdomens to the edge of the media droplet using the forceps. Surface tension will help keep the tissue flat (**Figure 1F**).
NOTE: It is helpful for imaging to organize the abdomens in a column or row at this stage.
- Label a glass slide (i.e., control or experimental) and pick up the coverslip by slowly bringing the slide closer to the coverslip. Flip slide over and gently blot with a wipe to remove excess mounting media.
- Seal the edges of the coverslip with clear nail polish and repeat for all remaining experimental groups. Store slides in a slide box at 4 °C until ready to image.

6. Imaging and processing

- Image the fly abdominal wound area by first locating the melanin scar with a confocal microscope (**Figure 1B**), either a point scanner or a structured illumination (ApoTome) with a 40x oil or dry objective.
- Check the exposure on each channel, ensuring that the signal is below saturation. The imaging settings should be based on the brightest sample group. This is particularly important for ploidy analysis as the DAPI channel needs to stay in the linear range to accurately measure DNA content.
- Take a full z-stack image in all three channels with an optimal distance of at least 0.50 µm between slices. Save captured images and open the file in the image analysis program Fiji (also known as ImageJ).
- For each image, create a z-stack projection using the sum of slices option for all channels.
- Rotate the images as necessary to ensure the nuclei are lined up horizontally across images (**Figure 3A** and **Figure 4E**).

- Crop all the images to a rectangular selection of 300 μm x 300 μm centered around the wound site or center of uninjured control. Identify the area by drawing a rectangle and selecting **Edit | Selection | Specify**. Check that scaled units are in microns to ensure the same sized box is used for all images to be analyzed.

7. Endoreplication (ploidy) analysis

- Using Fiji, select the **Grh channel window** and duplicate the image. Then use the **threshold tool** to create a mask. Manually adjust the threshold by sliding the top bar to minimize background without causing the nuclei to shrink drastically (**Figure 4D**).
- If any nuclei in the Grh channel are touching in the threshold image, use the **paintbrush tool** (2 pixel width) in the same color as the background, to draw a line between the nuclei. Click to apply 1x when finished to generate the final mask.
- Generate a region of interest (ROI) map by using the **Analyze Particles** function: set size to 5 μm -60 μm in order to capture most of the nuclei without including the background.
- Manually adjust the ROI map as needed in the **ROI manager**. Delete any selections that are not nuclei and add any nuclei to the list that were not identified by outlining the nucleus with the freehand selection tool and adding it to the **ROI manager (Figure 4D)**.
- Select the **DAPI channel** then click **Show All** in the **ROI manager** to apply the generated ROI map in the Grh channel onto the DAPI channel.
- Delete any selections where the epithelial nuclei outline overlaps with nonepithelial nuclei (e.g., nuclei from muscle or fat) from the ROI map. Grainyhead only stains epithelial nuclei, whereas DAPI stains all nuclei. Check that each outlined selection contains only one nucleus and delete or edit any selections with more than one nucleus. Save edited ROI list.
- Measure the area and integrated density of each epithelial nuclei in the ROI map using the analysis tools in Fiji. Export the values into a spreadsheet program.
- Measure the average image background using the circular selection tool. Draw three circles that do not overlap with any nuclei in different areas of the DAPI image. Add the area and integrated density of each of the circles to a spreadsheet program to establish the background image brightness.
- Start by calculating the average background per unit area for each image by dividing each background integrated density value by its corresponding area. Then average the three integrated density per area measurements for the image in order to obtain the average background per unit area.
- Next, calculate the total background of each DAPI nucleus by multiplying the area of the nucleus by the average background per unit area. The normalized DAPI intensity for each nucleus measured can then be calculated by subtracting the total background of each nucleus from its measured integrated density.
- Average all the normalized DAPI intensity values from the uninjured epithelial control. The uninjured epithelial nuclei were previously calculated to have a ploidy value of 2C and can serve as a reference for calculating ploidy in the epithelial nuclei from the experimental conditions³.
- Calculate the ploidy of each nucleus by dividing the normalized DAPI intensity of each nucleus by the normalized value from reference uninjured epithelial control (2C), then multiply the value by 2 to equal the normalized ploidy (C-value):
(Nuclear Integrated Density - Background Nuclear Integrated Density)/Average Nuclear Integrated Density (uninjured epithelial nuclei = 2C) x 2 = epithelial nuclear ploidy (C)
- Graph nuclei with ploidy values as a dot plot, histogram, or grouped into a bar graph accordingly (i.e., 2C [0.6-2.9C], 4C [3.0-5.9C], 8C [6.0-12.9C], 16C [13.0-24.9C], and >32C [$>25.0\text{C}$] (**Figure 3F**).

Representative Results

A detailed protocol is provided to use *D. melanogaster* as a model to study wound-induced polyploidization (WIP). This wound healing model provides many advantages over mammalian and other fly models of WIP. Polyploidy was easily induced by a mechanical puncture with an insect pin and polyploid cells were generated within a short period of time (2-3 dpi) (**Figure 1A, 1B**)⁴. The major challenge is the dissection of intact abdominal tissue without any perturbations to the epithelium. The *D. melanogaster* epithelium is easily accidentally bumped or scratched with the sharp dissection tools. Therefore, the steps of this protocol should be practiced prior to use and analysis.

First, the injury was restricted to the ventral female abdomen, which provides a large, flat opaque tissue area ideal for imaging. The puncture wounds were inflicted in the pleurite epithelium, which lies on either side of the ventral midline sternites and targeted between tergite (T) segments T4-T5 (**Figure 1A-C**). This wound placement provides a large visible area that is not disrupted by the dissection. Challenging steps include the abdominal spring scissor cut and pinning steps (**Figure 1D, 1E**). The spring cutting step worked best when the abdomens were cut in a reduced volume of Grace's solution (~30 μL) to decrease tissue movement. A well-centered cut along the dorsal midline was necessary to provide sufficient area on the abdominal dorsal flaps to pin open on the dissection plate (**Figure 1C**). The abdomen must be gently pinned on the four corners without excessive force (**Figure 1E**). A pin push that is too hard will distort the abdominal tissue and could even push the tissue into the dissection plate. If this happens, the tissue must be discarded. Once the abdominal tissue was fixed, it remained on the dissection plate until immunofluorescence staining was complete and the abdomens were mounted on a glass coverslip for imaging (**Figure 1F**).

Wound healing requires a continuous epithelial sheet to form, which is dependent on endoreplication and cell fusion^{4,16}. The septate junction protein FasIII, which labels cell-cell junctions, provided an indicator for whether any processing perturbations occurred during preparation (**Figure 1G, 1H**). Abdomens with large scratches (unstained area) that perturb the wound area must be discarded and were not used for further analysis (**Figure 1H**).

The next step was to analyze intact samples for any defects in WIP. This protocol includes distinct assays to detect different aspects of the WIP response (**Figure 2**). Wound repair was complete when a central, large, multinucleated cell covered the wound scab (**Figure 3A**). Here cell fusion was detected by staining for FasIII/Grh and quantifying the number of Grh⁺ epithelial nuclei encompassed in the FasIII outlined area⁴. Defects in wound closure or re-epithelialization were detected when gaps of >10 μm in the epithelial sheet were observed (**Figure 3B**, red arrow). This was the case, for example, when WIP was inhibited by the activation of mitotic cycle via expression of *stg, fzr^{RNAi}*, as recently reported¹⁶. In this genetic condition, 52% of the wounds were not able to form a continuous epithelial sheet over the wound scab (**Figure 3B, 3C**).

Another method to measure wound repair in this model was by visualizing the epithelial membrane with epi-Gal4 expression of UAS-mCD8-ChRFP⁴ (**Figure 2, Figure 3D**). In the control, 91% of epithelial wounds closed completely by 3 dpi, but inhibiting WIP by blocking endoreplication (*E2f1^{RNAi}*) and cell fusion (*RacDN*) simultaneously, as previously reported, caused 92% of epithelial wounds to remain completely open (**Figure 3D, 3E**)^{8,16}. The activation of mitotic cell cycle by expression of *stg, fzr^{RNAi}* also resulted in an epithelial wound closure defect. However, by visualizing the epithelial cell membrane, the extent of re-epithelialization defect could be determined. The WIP mutant (*E2f1^{RNAi}, RacDN*) fly wounds were more open than the *stg, fzr^{RNAi}* wounds (**Figure 3D**, dashed red outline)¹⁶. This membrane wound healing assay provided more information on the extent of the wound repair defect. As a result, re-epithelialization defects could be grouped as either completely open, partially closed (i.e., >10 μm gaps), or completely closed (**Figure 3D, 3E**).

In addition to cell fusion, epithelial cells grow in size by endoreplication, an incomplete cell cycle that doubles the nuclear DNA content. Endoreplication was assayed by both cell cycle activity and direct nuclear DNA ploidy measurements (**Figure 2** and **Figure 4**). Here, cell cycle activity was detected by incorporation of the thymidine analog, EdU (**Figure 4A, 4B**). *D. melanogaster* epithelial cells were found to enter the endocycle, an incomplete cell cycle that oscillates between the S and G phases without an intervening M phase^{4,12}. The adult *D. melanogaster* diet was supplemented with EdU⁺ food prior to injury and the flies were maintained on an EdU⁺ diet until dissection at 2 dpi (**Figure 4A**). The EdU was then detected using the manufacturer's Click-iT protocol. This EdU assay was used to determine where, when, and how many nuclei were triggered to enter S phase in response to a wound. Using the Gal4/ UAS system, it was recently found that epithelial specific expression of *myc* can either block (*myc^{RNAi}*) or exacerbate (*Myc* overexpression) the competence of epithelial cells to enter S phase. As result, it has been shown that *Myc* is sufficient to induce endoreplication in postmitotic cells, even without injury^{16,22}.

Next, epithelial ploidy was determined by directly measuring nuclear DNA content. Epithelial nuclei were identified by immunofluorescence staining for the epithelial specific marker, Grh (**Figure 4D**). In the Fiji imaging software, epithelial nuclei were systemically identified and then thresholded using Grh nuclear stain. Nuclei were then separated and the ROIs overlaid on to the SUM of stacks DAPI image (**Figure 4D, 4D**, green arrow). Any overlapping nuclei were manually deleted before the Integrated Density of the selected nuclei was measured (**Figure 4D, 4D**, red arrows). This semiautomated method allows one to quantify the distribution and ploidy of most nuclei throughout the uninjured and repaired fly abdominal epithelium⁸. As recently reported, the epithelial nuclei surrounding the wound were composed of 44% polyploid nuclei with DNA content more than 3C at 3 dpi (**Figure 4E, 4F**)¹⁶. As expected from the EdU results, knockdown of *myc* led to a significant block in endoreplication, as only 9% of epithelial nuclei were polyploid, whereas overexpression of *Myc* resulted in 100% polyploid epithelial nuclei around the wound site (**Figure 4F**)¹⁶. Epithelial nuclear size was also visibly affected by *myc* expression with either reduced or enlarged nuclei present. However, nuclear area is not an accurate measure of ploidy and physiological effects, because factors such as cell stretching can also influence nuclear size without affecting nuclear DNA content²⁰.

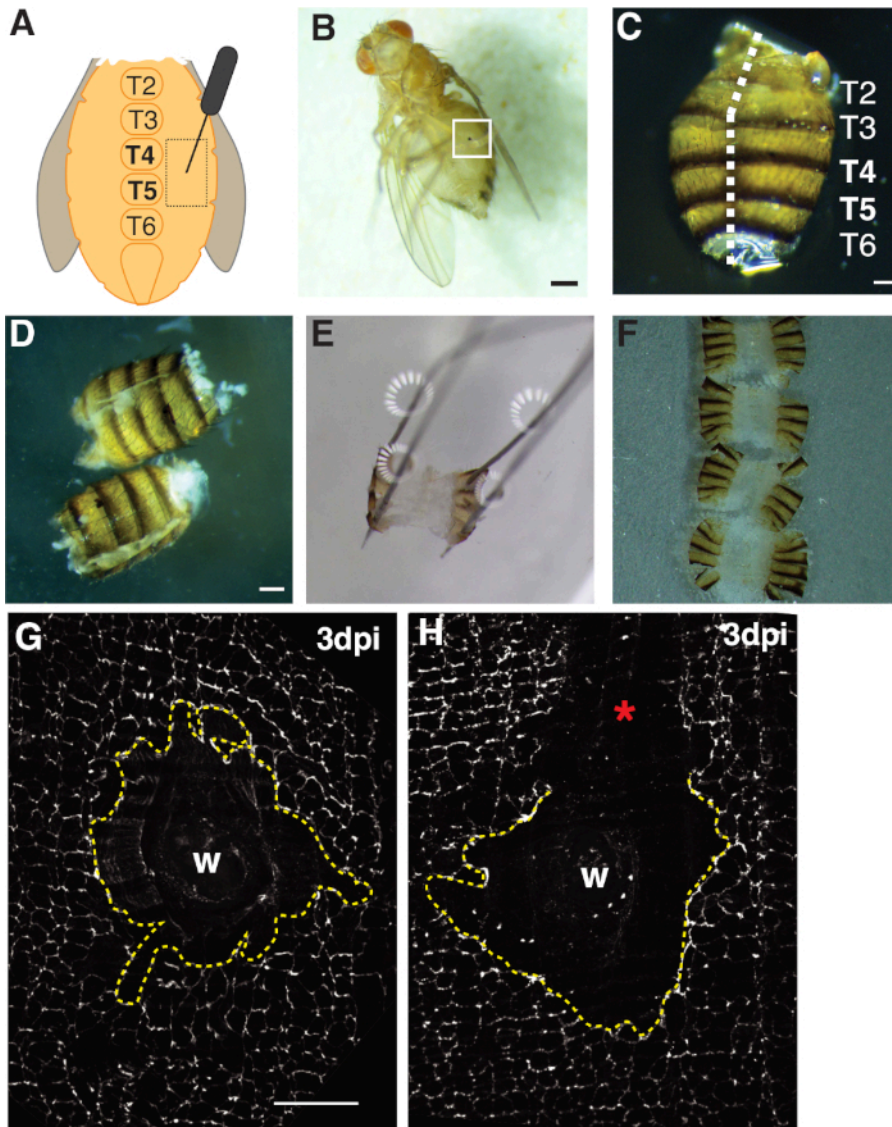


Figure 1: Adult fruit fly abdominal wounding, dissecting, and tissue mounting. (A) Diagram of the adult abdominal wounding assay. Flies should be injured on either side of the abdomen at tergite 4 (T4). (B) Adult female fruit fly 3 dpi with melanin scab formed from wound healing (white box). Scale bar = 50 μ m. (C) Dissected adult abdomen, dorsal view, with tergites labeled. Abdomens were filleted down the midline of the dorsal side (white dashed line). Scale bar = 50 μ m. (D) Dissected and filleted adult abdomens prior to pinning. Scale bar = 50 μ m. (E) Pinned adult abdomen on a dissection plate. A pin was placed in each of the four corners of the abdomen on the dorsal side. The tissue was gently opened but not stretched, to avoid tearing. (F) Adult abdomens were mounted and placed on a glass coverslip with the inside of the abdomen facing down towards the coverslip and cuticle oriented toward the glass slide. (G) FasIII staining of intact wound area with no processing perturbation and a central syncytium (dashed yellow line). Scale bar = 50 μ m. (H) Image of a scratched wound area (*) with an unstained FasIII region that disrupts the syncytium. [Please click here to view a larger version of this figure.](#)

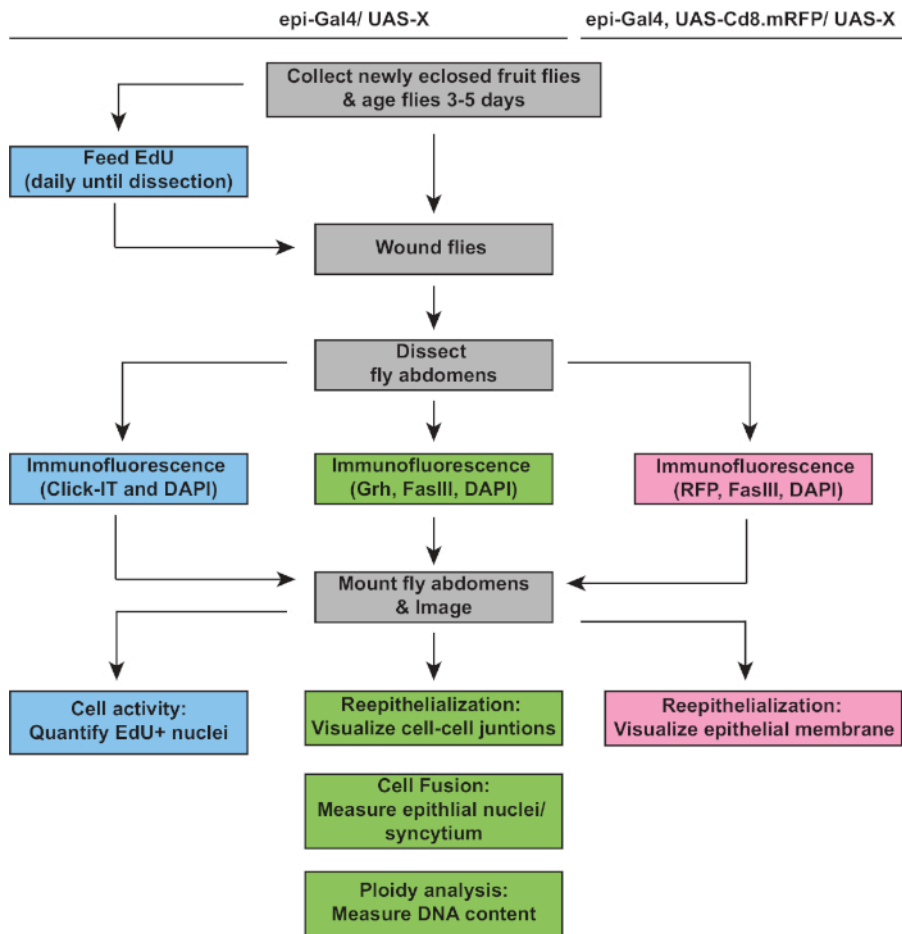


Figure 2: WIP analysis workflow. The flowchart depicts the three assays described in this study and overlapping and distinct steps to detect and measure the WIP response. The EdU assay measures cell cycle activity (blue boxes), ploidy and re-epithelialization are detected by Grh/ FasIII immunostaining (green boxes), and expression of membrane RFP allows measurement of the extent of epithelial wound closure (pink boxes). Common steps are in gray boxes and *D. melanogaster* strain genotypes are listed above. [Please click here to view a larger version of this figure.](#)

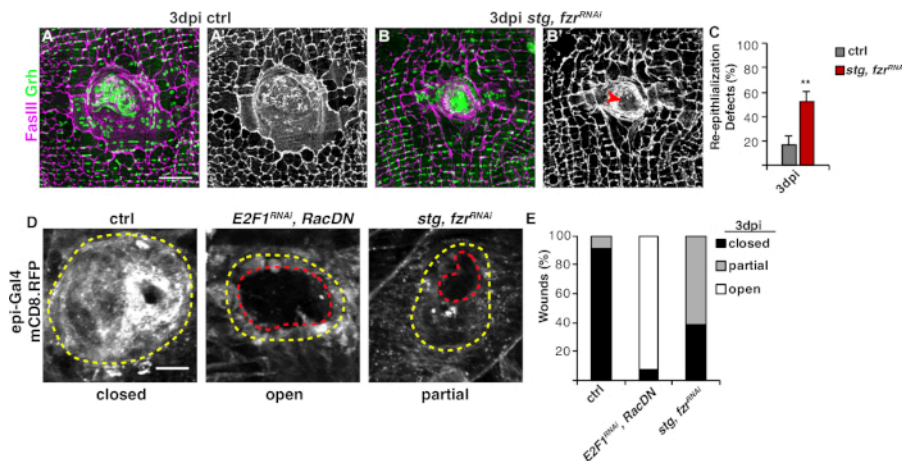


Figure 3: Methods to detect re-epithelialization during WIP. Re-epithelialization was perturbed when WIP was genetically inhibited. Immunofluorescent images of control (A) and *stg, fzr^{RNAi}* (B) at 3 dpi. Epithelial nuclei and septate junctions were stained with Grh (green) and FasIII (magenta), respectively. (A' and B') FasIII staining alone showed that re-epithelialization was impaired (red arrow) in *stg, fzr^{RNAi}* epithelium. Scale bar = 50 μ m. (C) Quantification of re-epithelialization defects (%) at 3 dpi (gray): control (n = 8), *stg, fzr^{RNAi}* (n = 6). Error bars indicate standard error; statistical significance was measured via Student's T-test, **P < 0.01. Re-epithelialization during wound repair could also be detected by expression of a membrane linked RFP using epi-Gal4, UAS-mCD8-RFP. (D) Immunofluorescent images of control, *E2F1^{RNAi}*, *RacDN*, and *stg, fzr^{RNAi}* at 3 dpi. Scale bar = 20 μ m. Wound scab (yellow outline) and open epithelial wound area (red outline). (E) Quantification of wound closure in ctrl (n = 11), *E2F1^{RNAi}*, *RacDN* (n = 13), and *stg, fzr^{RNAi}* (n = 13). Adapted from Grendler et al.¹⁶. [Please click here to view a larger version of this figure.](#)

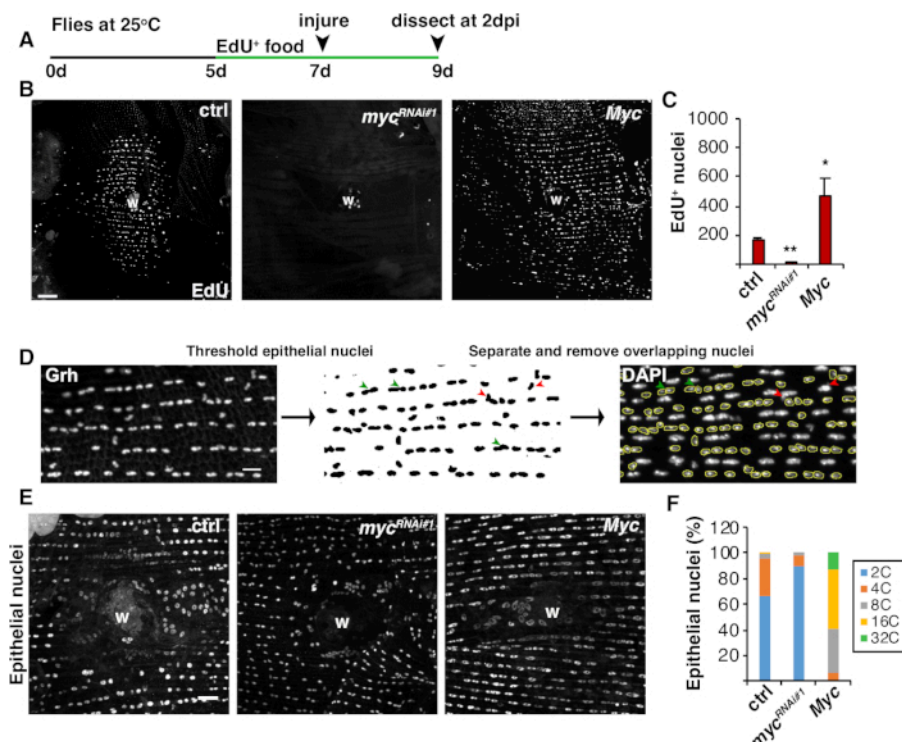


Figure 4: Methods to detect endoreplication during WIP. (A) Timeline of EdU assay: adult *Drosophila* were fed 75 µL of 5 mM yeast-EdU every day 2 days prior to injury and continued until 2 dpi. (B) Immunofluorescent images of EdU label in fly strains expressed with epi-Gal4/UAS system at 2 dpi. Wound scab (W). Scale bar = 50 µm. (C) Average number of EdU+ epithelial nuclei per fly at 2 dpi: ctrl (n = 37), *myc^{RNAi#1}* (n = 10), and *Myc* (n = 8). Error bars indicate standard error; statistical significance was measured via Student's T-test, *P < 0.05, **P < 0.01. (D) Schematic of detection and measurement of epithelial nuclear ploidy. Epithelial nuclei were identified and thresholded by the anti-Grh stain in Fiji. Overlapping epithelial nuclei were separated (green arrowheads) or removed (red arrowheads) if overlaid by nonepithelial nuclei. The integrated density and nuclear area of corresponding DAPI stained nuclei image were measured. (E) Epithelial nuclear size (Grh) was altered by *myc* expression at 3 dpi. (F) Epithelial nuclear ploidy (%) at 3 dpi: ctrl (n = 4), *myc^{RNAi#1}* (n = 6), and *Myc* (n = 3). Adapted from Grendler et al.¹⁶. Please click here to view a larger version of this figure.

Discussion

Presented is a detailed protocol on how to dissect and use the adult *D. melanogaster* abdominal epithelium to study how genes regulate WIP by altering re-epithelialization and endoreplication during wound repair¹⁶. Using this method, the proto-oncogene *Myc* was recently identified as a key regulator of WIP. *Myc* is required for epithelial cells to endoreplicate post injury and is sufficient for quiescent epithelial cells to endocycle both in adult fly epithelium and accessory glands^{16,22}. It was also found that switching epithelial cells to a mitotic cell cycle by expression of *stg*, *fzr^{RNAi}* is detrimental to wound repair. Continued studies using this method will identify other genes required to regulate re-epithelialization and endoreplication during WIP, revealing both similarities and differences to how polyploidy is regulated and functions in a variety of tissues.

This model and method offer unique advantages, including the easy induction of polyploidy with a mechanical puncture and the fact that polyploid cells are generated within days⁴. The tissue dissection and preparation protocols are based on larval dissection techniques²³, but the adult fly abdomen is more rigid and therefore easily perturbed. As a result, this protocol requires practice and precision to isolate an intact tissue to study WIP. Once dissected, however, the epithelium is clearly visible and easily imaged, yielding a snapshot of the wound healing process. This method provides a wealth of information on the adult fly's epithelial organization, cell and syncytium size, and the ploidy of cells and individual nuclei. While live imaging is not yet possible within the intact fruit fly due to its opaque cuticle, this protocol could be adapted to include currently available ex vivo culture conditions used in *D. melanogaster* to perform short-term live imaging studies²⁴.

In the future, this model will be ideal to study cell-to-cell crosstalk and the contribution of other cell types to WIP by regulating gene expression with the Gal4/UAS system in other cell types of interest. Similar questions can also be answered using a variety of genetic and mutant backgrounds. The dissected adult fly abdomen contains a variety of cell types that can be easily visualized using this method, including fat body and oenocytes, lateral muscle fibers, sensory neurons, trachea, and macrophage-like hemocytes. In addition, this model will allow researchers to investigate how physiological variables influence WIP, including sex, diet, infection, age, and environmental stressors. While the protocol uses the adult female fly due to its larger size, WIP also occurs in the male fruit fly (Gjelsvik and Losick, unpublished). Polyploid cells have been found to arise during aging and age-associated disease in the mammalian liver, brain, eye, and heart¹². The fruit fly model will enable researchers to study polyploidization in physiological and disease contexts because human disease-related genes are highly conserved.

Disclosures

None.

Acknowledgments

At Boston College, we would like to thank Dr. Eric Folker for use of his lab's camera and stereoscope microscope setup for imaging and Bret Judson at the Boston College Imaging Core for infrastructure and support. We would also like to thank the fly community resources: Bloomington Drosophila Stock Center (NIH P40OD018537), Vienna Drosophila Resource Center, and TRiP Center at Harvard Medical School (NIH/NIGMS R01-GM084947) for providing transgenic stocks used in this study. The mouse FasIII antibody were obtained from Developmental Studies Hybridoma Bank supported by NICHD of the NIH and maintained at The University of Iowa, Department of Biology, Iowa City, IA. Research reported in this publication was supported by the National Institute of General Medical Sciences of the National Institutes of Health under Award Number R35GM124691. The content is solely the responsibility of the authors and does not necessarily represent the official views of the National Institutes of Health.

References

1. Abreu-Blanco, M. T., Verboon, J. M., Liu, R., Watts, J. J., Parkhurst, S. M. Drosophila embryos close epithelial wounds using a combination of cellular protrusions and an actomyosin purse string. *Journal of Cell Science*. **125** (Pt 24), 5984-5997 (2012).
2. Wood, W. et al. Wound healing recapitulates morphogenesis in Drosophila embryos. *Nature Cell Biology*. **4** (11), 907-912 (2002).
3. Galko, M. J., Krasnow, M. A. Cellular and genetic analysis of wound healing in Drosophila larvae. *PLoS Biology*. **2** (8), E239 (2004).
4. Losick, V. P., Fox, D. T., Spradling, A. C. Polyploidization and cell fusion contribute to wound healing in the adult Drosophila epithelium. *Current Biology*. **23** (22), 2224-2232 (2013).
5. Wang, Y. et al. Integrin Adhesions Suppress Syncytium Formation in the Drosophila Larval Epidermis. *Current Biology*. **25** (17), 2215-2227 (2015).
6. Ramos-Lewis, W., LaFever, K. S., Page-McCaw, A. A scar-like lesion is apparent in basement membrane after wound repair in vivo. *Matrix Biology*. **74**, 101-120 (2018).
7. Lee, C. W., Kwon, Y. C., Lee, Y., Park, M. Y., Choe, K. M. cdc37 is essential for JNK pathway activation and wound closure in Drosophila. *Molecular Biology of the Cell*. **30** (21), 2651-2658 (2019).
8. Losick, V. P., Jun, A. S., Spradling, A. C. Wound-Induced Polyploidization: Regulation by Hippo and JNK Signaling and Conservation in Mammals. *PLoS One*. **11** (3), e0151251 (2016).
9. Tamori, Y., Deng, W. M. Tissue repair through cell competition and compensatory cellular hypertrophy in postmitotic epithelia. *Developmental Cell*. **25** (4), 350-363 (2013).
10. Xiang, J. et al. EGFR-dependent TOR-independent endocycles support Drosophila gut epithelial regeneration. *Nature Communications*. **8**, 15125 (2017).
11. Cohen, E., Allen, S. R., Sawyer, J. K., Fox, D. T. Fizzy-Related dictates A cell cycle switch during organ repair and tissue growth responses in the Drosophila hindgut. *Elife*. **7**, e38327 (2018).
12. Gjelsvik, K. J., Besen-McNally, R., Losick, V. P. Solving the Polyploid Mystery in Health and Disease. *Trends in Genetics: TIG*. **35** (1), 6-14 (2019).
13. Cao, J. et al. Tension Creates an Endoreplication Wavefront that Leads Regeneration of Epicardial Tissue. *Developmental Cell*. **42** (6), 600-615 e604 (2017).
14. Zhang, S. et al. The Polyploid State Plays a Tumor-Suppressive Role in the Liver. *Developmental Cell*. **44** (4), 447-459 e445 (2018).
15. Lazzeri, E. et al. Endocycle-related tubular cell hypertrophy and progenitor proliferation recover renal function after acute kidney injury. *Nature Communications*. **9** (1), 1344 (2018).
16. Grendler, J., Lowgren, S., Mills, M., Losick, V. P. Wound-induced polyploidization is driven by Myc and supports tissue repair in the presence of DNA damage. *Development*. **146** (15), 173005 (2019).
17. Mehrotra, S., Maqbool, S. B., Kolpakas, A., Murnen, K., Calvi, B. R. Endocycling cells do not apoptose in response to DNA rereplication genotoxic stress. *Genes & Development*. **22** (22), 3158-3171 (2008).
18. Patterson, M. et al. Frequency of mononuclear diploid cardiomyocytes underlies natural variation in heart regeneration. *Nature Genetics*. **49** (9), 1346-1353 (2017).
19. Gonzalez-Rosa, J. M. et al. Myocardial Polyploidization Creates a Barrier to Heart Regeneration in Zebrafish. *Developmental Cell*. **44** (4), 433-446 e437 (2018).
20. Webster, M., Witkin, K. L., Cohen-Fix, O. Sizing up the nucleus: nuclear shape, size and nuclear-envelope assembly. *Journal of Cell Science*. **122** (Pt 10), 1477-1486 (2009).
21. Knouse, K. A., Lopez, K. E., Bachofner, M., Amon, A. Chromosome Segregation Fidelity in Epithelia Requires Tissue Architecture. *Cell*. **175** (1), 200-211 e213 (2018).
22. Box, A. M. et al. Endocycles support tissue growth and regeneration of the adult Drosophila accessory gland. *bioRxiv*. 719013 (2019).
23. Karim, M. R., Moore, A. W. Morphological analysis of Drosophila larval peripheral sensory neuron dendrites and axons using genetic mosaics. *Journal of Visualized Experiments*. (57), e3111 (2011).
24. Dai, W., Montell, D. J. Live Imaging of Border Cell Migration in Drosophila. *Methods in Molecular Biology*. **1407**, 153-168 (2016).